

A Case Study on Sintering Characteristics of Yttria Stabilized Zirconia Powder Prepared by Two-Fluid Spray Drying

Jin Sam Choi[†] and Young-Min Kong^{*‡}

Department of Ceramic Engineering, Gyeongsang National University, Jinju 52828, Korea

**School of Materials Science and Engineering, University of Ulsan, Ulsan 44610, Korea*

(Received December 9, 2015; Revised March 11, March 28, 2016; Accepted March 29, 2016)

ABSTRACT

As a case study on yttria stabilized zirconia ceramics, the sintering characteristics of submicron powders and the granulation prepared by two-fluid spray drying of submicron particles were investigated. As-received powders of yttria stabilized zirconia particles were reduced to a uniform size of less than about 200 nm by repeated milling. Granulation size obtained by the two-fluid spray drying was affected by the organic matter and the primary particle size. Sintering behavior such as porosity, water absorption ratio, density, and transparency was influenced by processing conditions of the powder, and the discontinuous interfaces in a green body were reduced.

Key words : *Submicron powder, Two-fluid spray, Granule morphology, Transparency, Full density*

1. Introduction

Fundamental studies on the forming process which affects ceramic sintering behavior and the powder processing techniques to enhance a forming packing factor have been the object of interests. Particularly, since the forming process has direct effects on closed voids, density, microstructure, and grain boundary, etc. its importance in ceramic components requiring reliability is being increased.¹⁾ The studies on forming equipment and powder processing methods to improve formability of powders are well known. The former has been developed from uniaxial forming through triaxial isostatic press to hot isostatic press.²⁾ The latter involves a study of inducing uniform thermal conduction and an increase in sintered densities by improving friability and flowability through granulation of powders.³⁾ This is a method of manufacturing spherical granules with the solid contents only by evaporating the liquid phase with dry heat of 100 ~ 250°C when a mixed suspension of solid phase and liquid phase is passing through an atomizer. Depending on spray conditions, several shapes such as distorted sphere, apple, and doughnut, etc. are observed.⁴⁾ Granules from nozzle type and disk type of spray methods utilized by the industry have a size of about 10 ~ 100 μm, and spherical mixtures of fine particles, medium particles, and coarse particles are preferred in the forming process.⁵⁾ Meanwhile, in

the studies on sintering characteristics of yttria-stabilized zirconia (YSZ) granules using the spray pyrolysis method and on application of fillers, thermal insulators, and catalysts using silica hollow spheres of ~ 5 μm, it was considered to be dependent only on the process variables, and unrelated to the primary particle size of powders.^{6,7)} Also, since spray-dried bodies differed in pH change as a function of fed amounts of the precursor, sedimentation according to specific gravities, transferred amounts of suspension, spray method, and process variables such as drying heat temperature as a function of added organics and in application scope, derivation of a common denominator for the effects of primary particles is not easy. Nevertheless, the packing behavior as a function of particle sizes used in the granule preparation together with the particle surface area have an effect on the sintering characteristics. In ceramic powders, primary particles and submicron-sized secondary particles are agglomerated. Although deformation is easily caused in most agglomerated particles when stresses are applied to the particles, strongly agglomerated secondary particles maintain their agglomerated shapes. Since the green compact containing secondary agglomerated particles produces discontinuous microstructures at the interface of agglomerated zones to show a difference in heat transfer, its evasion is desirable.⁸⁾ Also, when the resin is filled with ceramic particles of 1 ~ 2 μm, the normal packing factor of the composite body is only 50%. In the case of ideal spherical particles synthesized by a chemical method, the packing factor is 75%, approaching the theoretical value.⁹⁾ This means that the size and the shape of ceramic particles are important elements acting as a driving force contributing to the packing factor and the reduction behavior of particle surface areas in the sintering process. From such viewpoint, when

[†]Corresponding author : Jin Sam Choi

E-mail : jinsamchoi@yahoo.co.kr

Tel : +82-55-752-8091 Fax : +82-55-772-1682

[‡]Corresponding author : Young-Min Kong

E-mail : longmin2@ulsan.ac.kr

Tel : +82-52-259-2722 Fax : +82-52-259-1688

ceramic powders are induced in a nano scale, attention has been paid to the fact that the particles are changed to have a spherical form to reduce the surface area along with the possibility of a change in the sintering characteristics due to suppression of discontinuous interfaces between particles by an increase in powder density per unit volume and in forming packing factor when these particles are granulated. For application of this idea to YSZ, a uniform particle distribution was induced in the bulk powders, followed by preparation of granules by the two-fluid spray known to have advantages useful for granulation of submicron particles.^{10,11)} Through comparisons between the sintered body of the granules and that of the uniform submicron powder in shrinkage rate, sintered density, base transmittance, etc. evaluations were made as a foundation study on the sintering behavior per case as a function of powder processing methods.

2. Experimental Procedure

Ytria-stabilized zirconia as a starting material provided by the manufacturer, ZrO₂ balls (0.3 mm, Nikato, Jp), and IPA(Iso Propyl Alcohol, Sigma-Aldrich, US) in a volumetric ratio of 1 : 2 : 3 were fed into a teflon pot with a size of 90 × 210 mm (diameter × length). At this time, the total capacity did not exceed 70% of the pot volume. The slurry in this pot which had been wet-milled for 14 days at a rotating speed of 260 ~ 290 rpm/ min(deceleration ratio 5 : 1 for 1600 rpm/min) was dried at 45°C for 24 h, and used as powders for the control group and the granule preparation.¹⁰⁾ Tap density(powder mass/powder final apparent volume) and Hausner ratio(tap density/apparent density) were obtained by the constant mass procedure after powder tapping of 2,000 times was repeated for 3 times. The instrument used at this time was a tap density tester (JV200, Copley, UK) (Fig. 1(a)). 20 g of pulverized powder and 250 cc of distilled water were placed in a beaker and dispersed for 10 h at the speed of 32 × 10³ rpm/min by using a disperser (IKA, T25, US). Forming agent, plasticizer, lubricant, dispersing agent, antifoaming agent, etc. of Table 1 were then added to this slurry, followed by agitation and dispersion for 24h. After being left unattended at 25°C for 24 h, this slurry was fed into a two-fluid spray dryer (SD-Basic, Lab Plant, UK). At this point, dispersion and agitation was conducted to prevent sedimentation of solid contents until the slurry

transfer was terminated (Fig. 1(b)). Spray drying conditions were 180°C, 120°C, 5.5 bar, and 20 μm for inlet temperature, exit temperature, air pressure, and orifice diameter, respectively.

1.50 g of prepared granules was subjected to the primary forming in a cylindrical mold of 12 mm at the pressure of 25 MPa, and then placed in the rubber tube for removal of inside air by a vacuum pump, followed by isostatic pressing (ISA-CIP-0050-0200-30, Ilshin, Kr) at the pressure of 200 MPa and normal sintering at 1450°C for 6 h. Specimens for the control group were also prepared by the same method. Crystal phases of the powders were observed using XRD (D/MAX-2250V, Rigaku, Jp), while porosity, water absorption ratio, true specific gravity and apparent density, etc. of the sintered specimens were measured according to the KS L3114 method. Base transmittance of sintered specimens was compared by photographing with a digital camera (800 px) at 600 Lux on a vision color sample composed of 2 upper and lower lines of 2 mm in black color and 1 center line in red color. Microstructures of the specimens were observed using SEM/EDS (JSM-6700F, Jeol, Jp) after fine polishing of the surfaces with abrasive papers and diamond paste (0.2 μm).

3. Results and Discussion

Figure 2 shows a particle size distribution, a microstructure, and a crystal phase. In Fig. 2(a) showing the particle

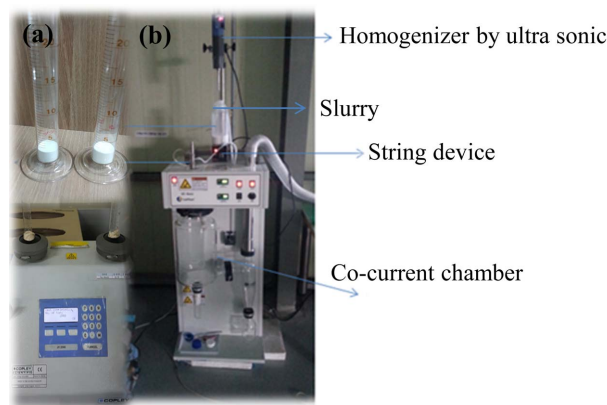


Fig. 1. Photos of (a) the tapped density tester and (b) two-fluid spray dryer used in this study.

Table 1. Slurry Formulations for Two-Fluid Spray Drying

Component	Type	Amount
Polyethylene glycol ¹⁾ (P.E.G-20000)	Binder or Green body strength	0.3 wt%
Ethylene glycol ²⁾	Plasticizer and Rheology	2cc
Triton X-100 ³⁾	Dispersant	1cc
SN5485 ⁴⁾	Lubrication role	1cc
Glycerol ⁵⁾	Surface tension	5cc
Fish Oil ⁶⁾	Charge net and Anti-forming	1drop

¹⁾Sanyo Chem., Jp, ^{2,3)}DaeJung Chem., Kr, ⁴⁾Sanokopu, Kr, ⁵⁾Junsei Chem., Jp ⁶⁾Sigma-Aldrich, US

size distribution, $D_{50} = 2 \mu\text{m}$ and $D_{90} = 10 \mu\text{m}$, while the microstructure of bulk powders with acicular and square-shaped small particles being agglomerated to coarse particles and the XRD crystal phase was observed to be zirconium oxide ($\text{Zr}_{0.96}\text{Y}_{0.03}\text{O}_{1.98}$) in Figs. 2(b) and (c).

In general, oxide particles have a difference in specific surface areas depending on particle shapes such as irregular shape, rhomboid shape, spherical shape, etc. and are known to be difficult to pulverize to particles smaller than $1 \mu\text{m}$ by simple impact force alone as particle pulverization apparatus of compression force, impact force, frictional force, shear force, flexure force. However, in the present study, uniform spherical particles smaller than $\sim 100 \text{nm}$ were observed in Fig. 3 for observation of the microstructure of particles following pulverization for 14 days, while Zr and Y elements were affirmed to be the main composition according to the EM/EDS analysis. In the studies on preparation of uniform, nano-scale amorphous powders, this was attributed to the change of the friction force between pulverization media to the energy for forming new surfaces upon formation of the condition where 0.3mm ZrO_2 balls as a pulverization medium did not interfere with rotation by rotation of the mill shaft.^{10,12} At the maximum rpm without action of centrifugal forces, pulverizing balls have self rotation in mutually opposite directions. If the particles are

positioned between these rotations at this time, pulverization of particles occur by the friction forces produced. Namely, when a surface tension rather than a shear stress is applied to atoms on the surfaces of the solid particles, deformation for formation of new surfaces may be considered to occur by reversible work acting as a compressive or tensile stress. Therefore, since only a part of individual atoms on the surface is surrounded by other atoms, an increase in new energy due to cutting of bonds occurs when atoms are moved from the inside to the surface by an external stress. Formation of uniform fine particles was considered to be accelerated by this force. Such tendency was also observed in a pulverization study for uniform nano-scale amorphous powders.¹⁰

In Fig. 4 where the granule shapes from two-fluid spray were investigated, the granules were observed to have a spherical shape of $1 \sim 10 \mu\text{m}$ in size. The granule sizes were determined by rotating speeds of the atomizer in the case of rotary atomizer method, while they are known to be determined in the dependence on pressure differences of the orifice in the case of pressure nozzle method. The sizes of these granules are $10 \sim 100 \mu\text{m}$, while they were about $3 \sim 10 \mu\text{m}$ for the two-fluid.^{11,13} Average particle size, D_p , in an algebraic probability distribution for the two-fluid granules is shown by the following equation.⁴

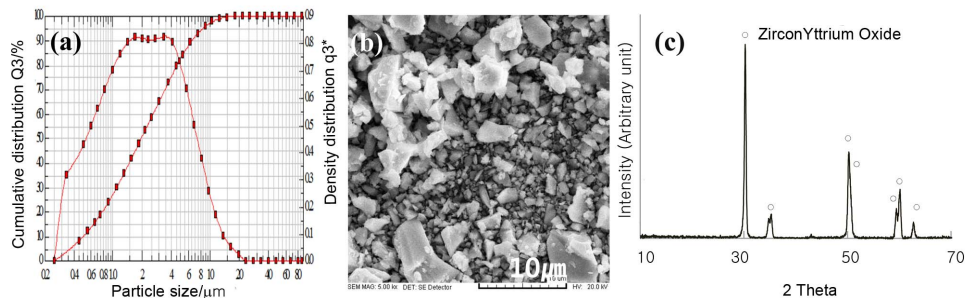


Fig. 2. As-received powder provided by supplier; (a) Particle size distribution, (b) Morphology of particles, and (c) XRD pattern.

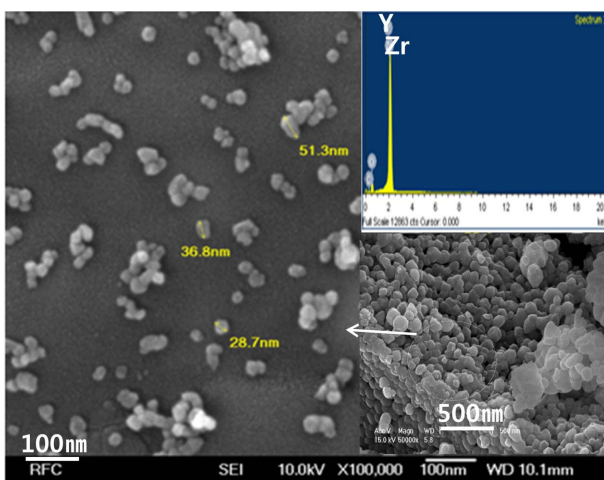


Fig. 3. SEM images and EDS spectra of zirconia milled for 14 days.

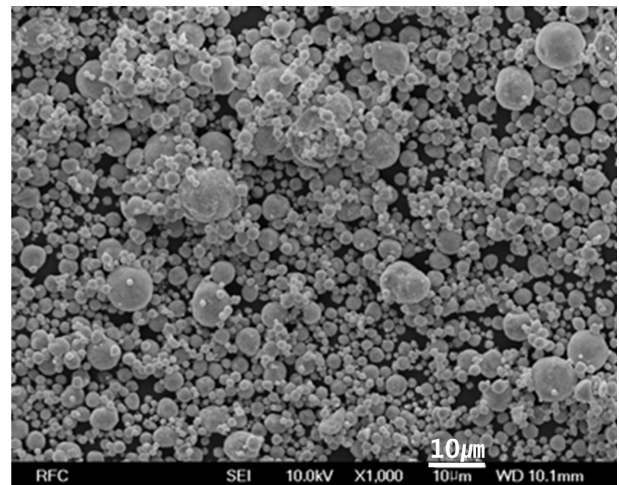


Fig. 4. SEM image of ZrO_2 granules obtained by two-fluid spray drying.

$$D_p = \frac{585\sqrt{\sigma}}{\mu\sqrt{\rho_L}} + 597\left(\frac{\mu}{\sqrt{\rho_L\sigma}}\right)^{0.45}\left(1000\frac{Q_L}{Q_n}\right)^{1.5} \quad (1)$$

where σ is the surface tension (dyne/cm), μ the viscosity (poise), ρ_L the liquid viscosity (g/m^2), Q_L the liquid flux (m^3/sec), and Q_n the gas flux (m^3/sec), respectively. In the equation (1), ρ_L and Q_L are constant when the slurry passes through the orifice hole. Therefore, the major factor having direct effects on D_p for the same batch can be seen to be the Q_n term. However, small granules smaller than $3 \mu\text{m}$ are considered to form due to an increase of the σ term dependent on the change in μ and the primary particle size due to P.E.G (Polyethylene glycol) base rather than Acrylic base.¹¹⁾ Therefore, the change in viscosities due to particle distribution of the starting material and the binder used may be seen to a secondary factor affecting granule sizes.

Figures 5(a) and (b) show the measured results of water absorption ratio and apparent porosity for sintered specimens. Water absorption ratios for the control group and the sintered specimen using two-fluid granules were shown to be 1.00% and 0.1%, and apparent porosities 1.5% and 0.2%, respectively. In Fig. 6(a) showing firing shrinkage rates for the sintered bodies, the shrinkage rate after sintering of the control group was observed to be 15%. In Fig. 6(b) for measurement of specific gravities, the specific gravity for the two-fluid sintered specimens was 5.99 g/cm^3 , approaching the theoretical density (6.05 g/cm^3). This is attributed to a difference between the particle growth rate accompanying sintering processes and the porosity annihilation rate due to a difference in forming packing factors although the particle sizes of two specimens were similar.¹⁴⁾ In general, the driving force for solid-state sintering can be explained by the matter transfer due to lattice diffusion caused by a difference in free energies between the free surface and the neck region in contact with the adjacent particle.¹⁵⁾

$$\Delta L/L_0 = (K\gamma a^3 D^* t/kTd^n) \quad (2)$$

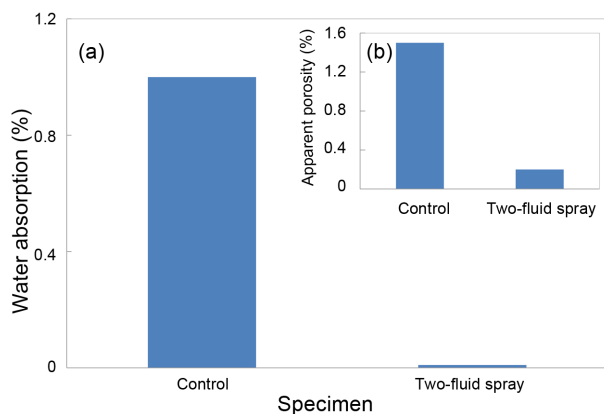


Fig. 5. Influence of treatment condition on YSZ powder. Relationship between (a)The apparent porosity, and (b) Water absorption of specimen sintered at 1450°C for 6 h in air.

where $\Delta L/L_0$ means the linear shrinkage corresponding to the sintering rate, γ the surface energy, a^3 the atomic volume for lattice vacancy, D^* the self-diffusion coefficient, k the Boltzmann constant, T the absolute temperature (K), d the particle diameter with the starting particles assumed to be identical, t the time, and K the constant dependent on the geometrical shapes while the exponent n is 3, and m about $0.3 \sim 0.5$. Although the equation (2) does not consider particle growth, an increase in sinterability may be inferred by affecting the diffusion coefficient and the temperature in an exponential relation when the a^3 term is increased, since the forming packing factor for the two-fluid specimens can be asserted to be relatively higher. Since the particles with a high specific surface area have a high surface free energy, thermodynamic driving force for reduction of the surface areas is great at low temperatures also. Thus, the claim that an improvement in nonuniform boundary regions due to particle agglomeration and an increase in specific surface areas due to spherical particles contribute to densification can be seen to be valid in the sintered density behavior of the two-fluid specimens. Such tendency is similar to the current study results as the sintered densities for particles smaller than $1 \mu\text{m}$ (surface area larger than $10 \text{ m}^2/\text{g}$) were higher than 95% in a study for observing the sintered density behavior of silicon nitride although the sintered densities for $3 \mu\text{m}$ particles were about 90%.¹⁶⁾ Hausner ratio for the tap density of powders obtained by the constant mass method was changed from 1.37 (a poor level, control group) to 1.03 (the best level, two-fluid granules). Consequently, this behavior can become a basis allowing determination that two-fluid contributes to an improvement of the sintering characteristics. In general, reduction of forming porosities or addition of sintering aids is known to enable the sinterability to be improved. In the case of Al_2O_3 powder, the post-sintering porosity is 0.25% and the sintered particle size $3 \mu\text{m}$ when the forming porosity is 40%, while the post-sintering porosity is 2% and the sintered particle size $10 \mu\text{m}$, in the case of 50%, and the post-sintering porosity is

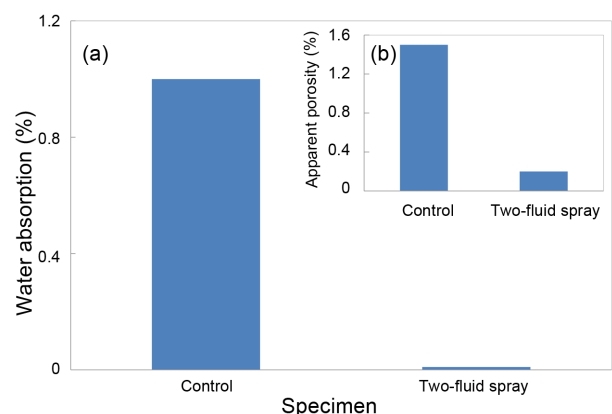


Fig. 6. Relationship between (a) Firing shrinkage, and (b) Specific gravity of specimen sintered at 1450°C for 6 h in air.

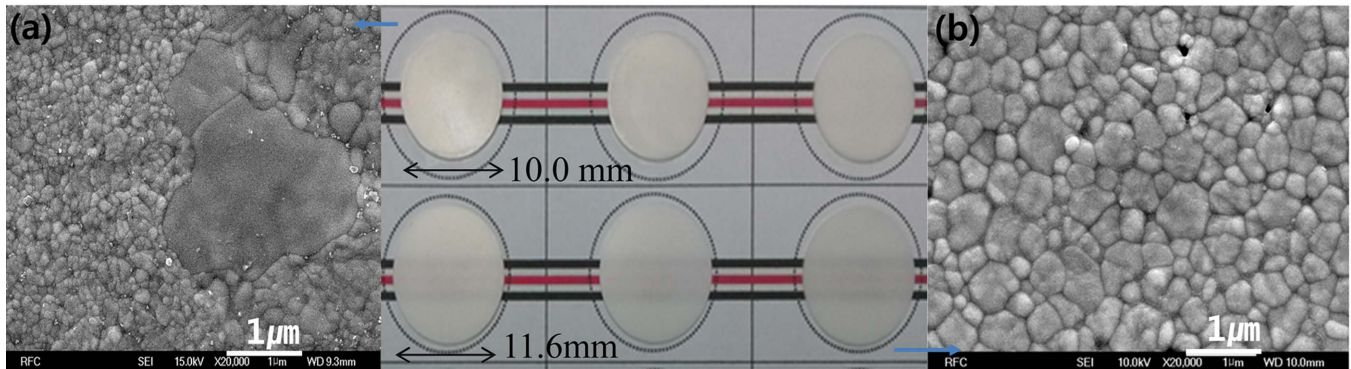


Fig. 7. SEM microstructure and transparency of sample obtained by (a) As-received, and (b) Two-fluid spray.

changed to 10% and the sintered particle size to 55 μm in the case of 60%.¹⁷⁾ In addition, when sintering aids are added to most ceramic powders, a change is known to occur in the sintered densities.¹⁶⁾ However, the results of the present study has shown that an increase in sintered densities is possible without incorporation of sintering aids if submicron particles are granulated.

Figure 7 shows a relative comparison of base vision colors and microstructures for the bulk powder and the two-fluid sintered specimen. Whereas abnormal growth particles due to agglomeration of the powder exist in Fig. 7(a), uniform crystal grains smaller than 0.5 μm are observed in Fig. 7(b). In general, transmittance is known to be drastically reduced due to scattering center action of visible light for the pores of 0.4 μm in size. This was in agreement with the tendency that transmittance was increased as 0.4 μm pores were annihilated in the sintering process for alumina powders having an average particle diameter of 0.3 μm .¹⁸⁾ Therefore, the sintered density and the transmittance are determined to be increased by an increase in forming packing factors per unit volume due to granulation of uniform primary particles and by an improvement in discontinuous interfaces between particles due to a decrease in porosities.

4. Conclusions

From the study on sintering characteristics of yttria stabilized zirconia particles and two-fluid granules using the same, the following conclusions have been derived.

Coarse particles and irregular particle shapes of the starting powders were changed to a uniform spherical shape smaller than 200 nm after pulverization. Size of the two-fluid spray granules was affected by the primary particle size and the viscosity of organics used.

Whereas the sintered bodies of the two-fluid spray granules with an improvement in forming packing factors per unit volume had reduction of forming porosities and discontinuous interfaces, the sintering characteristics were improved with the true specific gravity and the relative density being 5.99 g/cm^3 and 98.63%, respectively. In addition, since an increase in transmittance was exhibited due to

development of pores smaller than 0.2 μm and a uniform microstructure of about 0.5 μm , the two-fluid spray granules using submicron powders could be presented for a study on improvement of the sintering characteristics of yttria stabilized zirconia per case.

REFERENCES

1. Q. Nawaz and Y. Rharbi, "Various Modes of Void Closure during Dry Sintering of Close-Packed Nanoparticles," *Langmuir*, **26** [2] 1226-31 (2009).
2. T. Ekström, P. O. Käll, M. Nygren, and P. O. Olsson, "Dense Single-Phase β -Sialon Ceramics by Glass-Encapsulated Hot Isostatic Pressing," *J. Mater. Sci.*, **24** [5] 1853-61 (1989).
3. H. T. Laker, "Hot Isostatic Pressing of Ceramics," pp. 717-24 in *Hot Isostatic Pressing of Ceramics*, Vol. 65, Applied Sciences. Ed. By F. L. Riley, Springer, Berlin, 1983.
4. G. Bertrand, P. Roy, C. Filiatre, and C. Coddet, "Spray-Dried Ceramic Powders: A Quantitative Correlation between Slurry Characteristics and Shapes of the Granules," *Chem. Eng. Sci.*, **60** 95-102 (2005).
5. S. J. Lukasiewicz, "Spray-Drying Ceramic Powders," *J. Am. Ceram. Soc.*, **72** [4] 617-24 (1989).
6. Y. Ko, S. Lee, J. Kim, J. Lee, and Y. Kang, "Sintering Characteristics of Nano-Sized Yttria-Stabilized Zirconia Powders Prepared by Spray Pyrolysis," *J. Ceram. Proc. Res.*, **13** [4] 405-8 (2012).
7. H. Jang, H. Oh, J. Kim, and K. Jung, "Synthesis of Mesoporous Spherical Silica via Spray Pyrolysis: Pore Size Control and Evaluation of Performance in Paclitaxel Pre-purification," *Micro. Meso. Mater.*, **165** [1] 219-27 (2013).
8. C. A. Handwerker, P. A. Morris, and R. L. Coble, "Effects of Chemical Inhomogeneities on Grain Growth and Microstructure in Al_2O_3 ," *J. Am. Ceram. Soc.*, **72** [1] 130-36 (1989).
9. K. Zupan, D. Kolar, and M. Marinšek, "Influence of Citrate-nitrate Reaction Mixture Packing on Ceramic Powder Properties," *J. Power Sources*, **86** [1-2] 417-22 (2000).
10. J. Choi, "Rework Paste for Flip Chip Adhesion with Nanoscale Glass Frit(in Korean)"; Kr Patent 10-0928044 (November 16, 2009).
11. T. Iijima, "Two-Fluid Nozzle and Device Employing the

- Same Nozzle for Freezing and Drying Liquid Containing Biological Substances"; US Patent 6,148,536 (November 21, 2000).
12. A. K. Nath, C. Jiten, and K. C. Singh, "Influence of Ball Milling Parameters on the Particle Size of Barium Titanate Nanocrystalline Powders," *Phy. B: Con. Mater.*, **405** [1] 430-34 (2010).
 13. H. Kamiya, K. Isomura, G. Jimbo, and T. Jun-ichiro, "Powder Processing for the Fabrication of Si_3N_4 Ceramics: I, Influence of Spray-Dried Granule Strength on Pore Size Distribution in Green Compacts," *J. Am. Ceram. Soc.*, **78** [1] 49-57 (1995).
 14. S. Lowell, J. E. Shields, M. A. Thomas, and M. Thommes, "Characterization of Porous Solids and Powders: Surface Area, Pore Size and Density," *J. Am. Chem. Soc.*, **127** [40] 14117 (2005).
 15. W. D. Kingery, H. K. Bowen, and D. R. Uhlmann, "Introduction to Ceramics," pp.475-76 in *Grain Growth, Sintering, and Vitrification*, John Wiley & Sons, New Jersey, 1976.
 16. Y. Okamoto, N. Hirotsuki, M. Ando, F. Munakata, and Y. Akimune, "Effect of Sintering Additive Composition on the Thermal Conductivity of Silicon Nitride," *J. Mater. Res.*, **13** [12] 3473-77 (1998).
 17. J. G. J. Peelen and R. Metselaar, "Light Scattering by Pores in Polycrystalline Materials: Transmission Properties of Alumina," *J. App. Phys.*, **45** [1] 216-20 (1974).
 18. J. Klimke, M. Trunec, and A. Krell, "Transparent Tetragonal Ytria-Stabilized Zirconia Ceramics: Influence of Scattering Caused by Birefringence," *J. Am. Ceram. Soc.*, **94** [6] 1850-58 (2011).